PHYSICAL REVIEW E **67**, 050401(R) (2003)

Asphaltene nanoparticle aggregation in mixtures of incompatible crude oils

T. G. Mason[1] and M. Y. Lin[2]
[1]*Corporate Strategic Research, ExxonMobil Research and Engineering Company, 1545 Route 22 East, Annandale, New Jersey 08801*
[2]*Center for Neutron Research, NIST, Gaithersburg, Maryland 20899*
(Received 15 November 2002; published 21 May 2003)

We study the structure and phase behavior of asphaltenes comprised of large polyaromatic molecules in blends of naturally occurring crude oils using small angle neutron scattering (SANS). When two compatible oils are blended together, the asphaltenes remain dispersed as colloidal nanoparticles; however, when two incompatible oils are blended together, these asphaltene nanoparticles can aggregate to form microscale structures. We show that SANS directly probes asphaltene aggregation in unmodified (i.e., nondeuterated) crude oil mixtures due to a significant neutron scattering length density difference between the hydrogen-poor asphaltenes and the surrounding oil. Moreover, the small length scales probed by SANS are ideally suited for studying asphaltene aggregation: SANS simultaneously provides the average size and concentration of nanoscale asphaltene particles and also the volume fraction of microscale asphaltene aggregates. These discoveries yield a practical means for directly assessing the compatibility of crude oils and for diagnosing refinery fouling problems resulting from blending incompatible oils.

DOI: 10.1103/PhysRevE.67.050401 PACS number(s): 61.43.Hv, 64.70.Nd, 61.12.−q, 82.60.Qr

Asphaltenes are large hydrocarbon molecules comprised of fused polyaromatic ring cores; short aliphatic side chains typically adorn the rigid platelike cores [1]. Asphaltenes are believed to be formed from the geothermal decomposition of kerogen over many years [2]. Due to variations in the source kerogen and decomposition conditions, asphaltenes vary widely in molecular weight, structure, and heteroatom content. Most crude oils typically contain at least a few percent of asphaltenes; the high viscosity of heavy crude oils and tar sands arises from a much larger asphaltene content [1]. In most crude oils at room temperature and atmospheric pressure, asphaltenes exist as a stable colloidal dispersion of micelle-like association structures of a few asphaltene molecules [3]; we refer to these association structures as nanoparticles, since their sizes are typically 10 nm or less.

The interactions between asphaltene nanoparticles depend strongly on the relative abundance of smaller aromatic and aliphatic (or paraffinic) solvating molecules in the oil. If a heavier, predominantly aromatic oil containing many asphaltenes is blended into lighter, predominantly aliphatic crude oil containing few asphaltenes, some of the asphaltenes can aggregate into micron-scale or larger structures due to a reduction in the effective solvent quality for aromatic molecules. If this occurs, even over a small range of blending compositions, the blend is ''incompatible,'' otherwise it is ''compatible'' [4]. Refining incompatible blends is problematic because the aggregates can stick to process equipment, such as furnace walls, and form hard coke deposits. The continued coke buildup forces costly shutdowns [5]. These shutdowns cost the refining industry millions of dollars per year. Since heavier crude oils are becoming increasingly important as energy sources, understanding asphaltene aggregation in blends of crude oils is of great interest.

Traditional methods of detecting blend incompatibility range from spot tests on filter paper to direct optical microscopy observations of the aggregates. The strong optical absorption of visible light by asphaltenes and other molecules in crude oils has largely restricted light scattering studies to redispersed asphaltenes at dilute concentrations in nonabsorbing solvents [6]. Optical spectroscopy has been used to detect incompatibility in blends [7], but this method tells little about the relative concentrations and structures of asphaltenes in nanoparticles and aggregates. Small angle neutron scattering (SANS) has been used to examine asphaltenes recovered from crude oils and redispersed in synthetic deuterated oils [8]. However, using SANS to study asphaltene aggregation in blends of naturally occurring crude oils for the purposes of assessing compatibility has not yet been carried out. This may be due to the common, yet sometimes misleading, wisdom that deuterated solvents are required when performing SANS on hydrocarbon materials in order to reduce the incoherent scattering and also to achieve significant scattering contrast.

Here, we show that SANS is an excellent and useful probe of asphaltene structure and phase behavior in blends of naturally occurring, undeuterated crude oils. By performing SANS on both a compatible and an incompatible crude oil blend, we clearly demonstrate the hallmarks of aggregation in the scattered neutron intensity I as a function of wave number q. The most obvious indicator of incompatibility is the presence of a large surface scattering intensity from asphaltene aggregates at low q. A second indicator is the relative reduction in the strength of the scattering from micelle-like nanoparticles that have been incorporated into the aggregates. A third indicator is a reduction in the effective size of the nanoparticles that remain in solution after the aggregates have formed. We develop a physical model and semiempirical equation to fit the measured $I(q)$, and we show that this equation fits the data well for all blending volume fractions ϕ, defined as the volume of the heavier oil divided by the total volume of the heavier and lighter oils. This model is quite general and should apply to nanoparticle aggregation in a wide variety of contexts.

The compatible oils we blend are a heavier, asphaltene-rich Venezuelan crude oil (VACO) and a lighter, paraffinic Yemeni crude oil (YPCO). The incompatible oils we blend

 ©2003 The American Physical Society

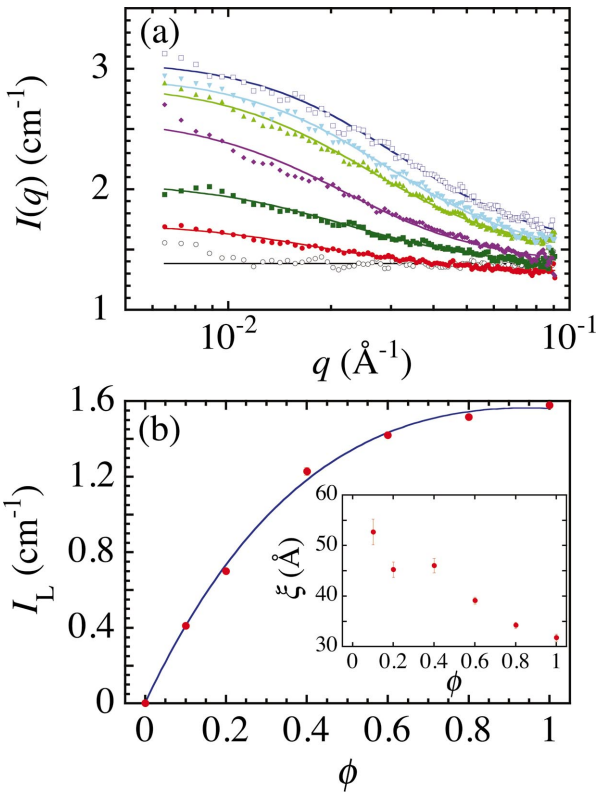

FIG. 1. (Color) SANS data showing soluble asphaltene nanoparticle structures in blends of compatible crude oils. (a) $I(q,\phi)$ for mixtures of VACO and YPCO at mixing volume fractions $\phi=0$, 0.1, 0.2, 0.4, 0.6, 0.8, and 1.0 in order from bottom to top. The solid lines are fits using Eq. (1). (b) The low-q scattering intensity associated with the Lorentzian term I_L as a function of ϕ obtained from the fits in part (a). The solid line is a fit of $I_L(\phi)$ to the hard sphere model, yielding an asphaltene volume fraction of $\phi_w \approx 0.14$ in pure VACO oil. Inset: the correlation length $\xi(\phi)$ of the asphaltene nanoparticles obtained from the fits in part (a).

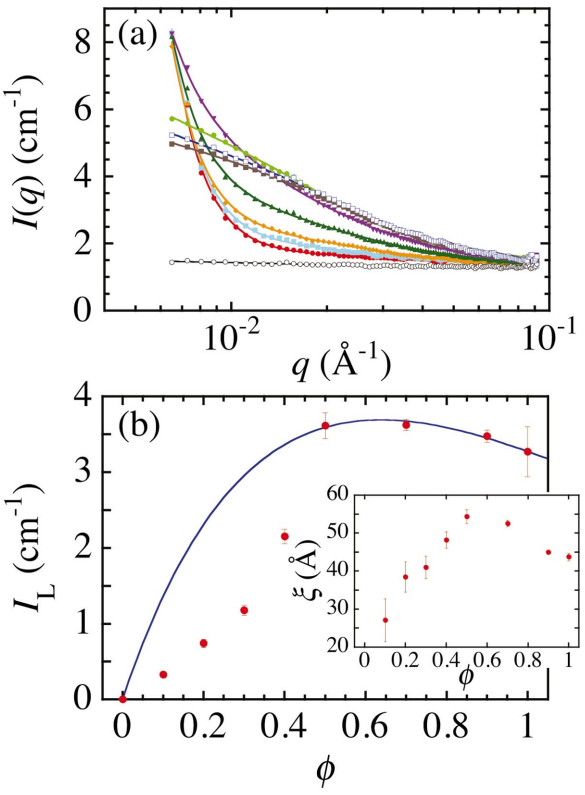

FIG. 2. (Color) SANS data showing asphaltene aggregate and nanoparticle structures in blends of incompatible crude oils. (a) $I(q,\phi)$ for mixtures of SACO and BPCO at volume fractions, $\phi=0$ (black open circles), 0.1 (red), 0.2 (light blue), 0.3 (orange), 0.4 (dark green), 0.5 (purple), 0.7 (light green), 0.9 (brown), and 1.0 (blue open squares) in order from bottom to top at $q=0.02$ Å^{-1}. The solid lines are fits using Eq. (1). (b) The Lorentzian scattering intensity $I_L(\phi)$ obtained from the fits in part (a). The solid line is a fit to data for $\phi \geq 0.7$ using the hard sphere model yielding $\phi_w \approx 0.20$. Inset: the correlation length $\xi(\phi)$ of the unaggregated asphaltene nanoparticles obtained from the fits in part (a).

are a heavier, asphaltene-rich Syrian crude oil (SACO) and a lighter, paraffinic British crude oil (BPCO). To allow for complete aggregation, all blends are made at least 15 days prior to measurement. Although waiting long after mixing permits us to look at the scattering from the equilibrium blends, it also allows asphaltene aggregates to sediment. To prevent the setting of aggregates from affecting our results, the samples are gently shaken prior to loading into 2-mm path length quartz cells. We have probed the blends using the NG7-SANS instrument at NIST's Center for Neutron Research. We have used the shorter end of the cold neutron spectrum, selecting a wave length $\lambda=5$ Å to minimize the attenuation due to hydrogen. All measurements have been performed at room temperature $T=23\,^{\circ}$C. The q range has been chosen so that a single measurement permits us to examine the asphaltene aggregates, nanoparticles, and incoherent scattering. A collection time of 30 min per mixture provides good statistics, yet is short enough that the sedimentation of the aggregates can be neglected.

The SANS $I(q)$ data for the VACO and YPCO blends are shown in Fig. 1(a). As ϕ is varied, the scattering functions for the mixtures lie systematically between the two limits for $I(q)$ for the unmixed, pure oils. The data for the SACO and BPCO blends are shown in Fig. 2(a). By contrast, these data do not lie systematically between the two limits for the pure crude oils. Instead, at the lowest $\phi=0.1$, there is a very sharp rise in $I(q)$ toward the lowest q. For successively higher $\phi=0.2$ and $\phi=0.3$, the same qualitatively sharp low-q rise in $I(q)$ is observed, although the overall magnitudes are successively lower. Even at $\phi=0.4$ and 0.5, there is a significant rise above the limit defined by pure SACO. For larger ϕ, the sharp rise in the low-q intensity disappears, and the $I(q)$ at $\phi=0.9$ lies completely inside the limit measured for SACO. For both pure paraffinic oils, YPCO and BPCO, $I(q)$ is flat, indicating that these oils contain very few asphaltenes.

To fit these data, we consider three distinct scattering contributions. First, because hydrogen nuclei occur in abundance in crude oils, there is a constant incoherent scattering, I_{incoh} that is independent of q. This intensity is generally proportional to the number of hydrogen nuclei per unit volume in the oil, since the scattering cross section for hydrogen dominates that of carbon [9]. Second, we include the coherent scattering from the asphaltene nanoparticles. Previous small

angle scattering measurements of fractionated asphaltenes dispersed in good solvents have revealed that $I(q)$ can be approximated by a Lorentzian: $I_L/(1+q^2\xi^2)$, where I_L is the low-q plateau intensity and ξ is a correlation length [10] that can be interpreted as the average Guinier radius of gyration of the particles, $\langle R_g\rangle_G = 3^{1/2}\xi$. Third, the surface scattering from asphaltene aggregates is modeled as a Porod-like power law: $I_{\mathrm{surf}}(q/q_1)^{-\alpha}$, where I_{surf} represents the surface scattering intensity at the lowest wave number q_1 in our measurement range and α is the power law exponent. For aggregate interfaces that are not perfectly sharp, the exponent is $\alpha = 4 + 2q_1^2 d^2$, where d is the length scale characterizing the interfacial diffuseness [11]. We sum these three contributions to obtain a semiempirical expression for the total intensity:

$$I(q) = I_{\mathrm{incoh}} + I_L/(1+q^2\xi^2) + I_{\mathrm{surf}}(q/q_1)^{-\alpha}. \qquad (1)$$

For incompatible mixtures, there are five fitting parameters that may vary with ϕ: I_{incoh}, I_L, ξ, I_{surf}, and α (q_1 is fixed). For compatible mixtures, there is a simple systematic progression of $I(q,\phi)$ between the limits of the two pure crude oils at $\phi=0$ and $\phi=1$, and $I(q,\phi)$ can be fit well using only I_{incoh}, I_L, and ξ in the first two terms in Eq. (1); the third term is not used for compatible mixtures since no surface scattering features in $I(q)$ are present to constrain the parameters I_{surf} and α. The true utility of Eq. (1) will be determined not just by the quality of the fits, but more importantly by the physical significance of how the fitting parameters vary over the full range of ϕ.

The fits to the measured $I(q,\phi)$ for the VACO-YPCO blends are shown in Fig. 1(a). Because these oils are compatible, there is no low-q rise in $I(q)$, and the data are fit well using only the first two terms of Eq. (1). A linear rise in $I_{\mathrm{incoh}}(\phi)$ from about 1.3 cm^{-1} at $\phi=0$ to about 1.5 cm^{-1} at $\phi=1$ is observed. In Fig. 1(b), $I_L(\phi)$ rises linearly from zero at low ϕ, yet the rise becomes progressively smaller for $\phi \geqslant 0.5$, indicating a negative curvature. In Fig. 1(b) inset, ξ continuously decreases from $\xi \approx 50$ Å at $\phi=0$ to $\xi=30$ Å at $\phi=1$.

By contrast, the fits to the measured $I(q,\phi)$ for the incompatible SACO-BPCO blends are shown in Fig. 2(a). All three terms in Eq. (1) are required to fit the data. The fits are excellent for all q and ϕ. We find that $I_{\mathrm{incoh}}(\phi)$ is constant at about 1.3 cm^{-1} for all ϕ. As shown in Fig. 2(b), $I_L(\phi)$ rises more sharply for $0.3 \leqslant \phi \leqslant 0.5$ than at lower ϕ, indicating a positive curvature. For higher ϕ, I_L for SACO-BPCO mixtures saturates or even decreases slightly. In Fig. 2(b) inset, we show $\xi(\phi)$ for the unaggregated asphaltenes in SACO-BPCO mixtures as a function of ϕ. By contrast to the compatible blends, ξ rises from around $\xi \approx 30$ Å at $\phi=0.1$ to a peak at $\xi \approx 50$ Å at $\phi=0.5$. For larger $\phi > 0.5$, ξ decreases in a manner similar to the compatible blends. The fitting parameters $I_{\mathrm{surf}}(\phi)$ and $\alpha(\phi)$ for SACO-BPCO mixtures are shown in Figs. 3(a) and 3(b), respectively. An abrupt increase in $I_{\mathrm{surf}}(\phi)$ occurs between $\phi=0$ and $\phi=0.1$. For larger ϕ, $I_{\mathrm{surf}}(\phi)$ decreases monotonically and continuously toward zero as $\phi \to 1$. The power law exponent $\alpha(\phi)$ is about 4.5 for $0.1 \leqslant \phi \leqslant 0.3$. This large exponent implies that the asphaltene aggregates have diffuse interfaces with a layer thickness that we estimate to be $d \approx 70$ Å. For larger ϕ, α decreases to about 3 at $\phi=0.5$, and drops toward zero rapidly thereafter.

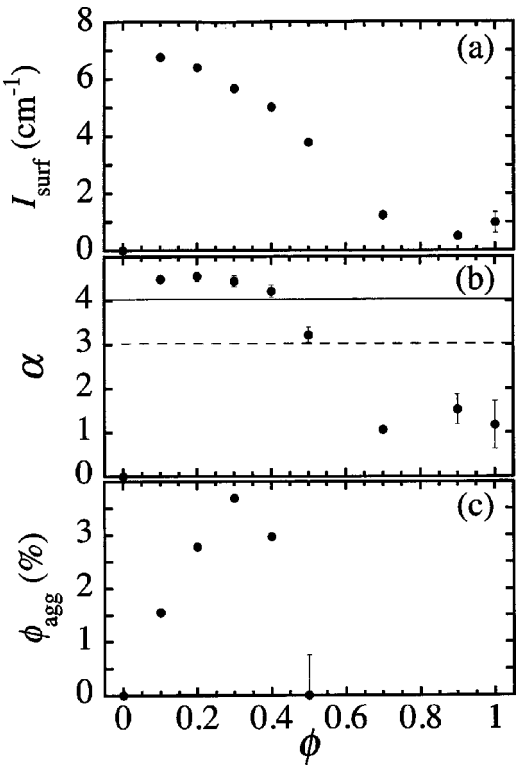

FIG. 3. (Color online) Primary indicators of asphaltene aggregation for SACO-BPCO blends. (a) The surface scattering intensity from asphaltene aggregates, I_{surf}, as a function of mixing volume fraction ϕ obtained from the fits to data in Fig. 2(a) using Eq. (1). (b) The power law exponent $\alpha(\phi)$ associated with surface scattering from asphaltene aggregates. The solid line at $\alpha=4$ represents Porod scattering from abrupt interfaces. The dashed line at $\alpha=3$ represents the lower bound for aggregates with fractal surfaces. (c) The volume fraction of aggregated asphaltenes, $\phi_{\mathrm{agg}}(\phi)$, deduced from the difference between the predicted $I_L(\phi)$ for unaggregated hard spheres and the measured $I_L(\phi)$ after aggregation in Fig. 2(b).

The linear rise in $I_L(\phi)$ at low ϕ for the compatible blend reflects a simple increase in the number of unaggregated asphaltene particles as more of the asphaltene-containing crude oil is added into the mixture. The saturation in $I_L(\phi)$ at high ϕ indicates that there are enough asphaltene particles in pure VACO to cause the low-q scattering intensity to depend on the relative proximity of particles through the structure factor $S(q,\phi_u)$ based on the Percus-Yevick (PY) closure [12,13], where ϕ_u is the volume fraction of unaggregated asphaltene nanoparticles in the mixture. This PY structure factor is valid at lower ϕ_u well below packing. The asphaltene-rich whole crude oil has an asphaltene nanoparticle volume fraction of $\phi_w = \phi_u(\phi=1)$. In Fig. 1(b), we fit the data for $I_L(\phi)$ to $I_c\phi\phi_w \lim_{q\to 0} S(q,\phi\phi_w)$, where I_c and ϕ_w are parameters; this captures the linear rise in $I_L(\phi)$ in the highly dilute limit and also the sublinear behavior caused by the structure factor at larger ϕ. In this fitting form, the product $\phi\phi_w$ represents the effective hard sphere volume fraction of asphaltene nanoparticles in the mixtures. Although the asphaltene nanoparticles may not behave as hard spheres either in shape or

interactions, the fit is excellent and allows us to estimate that pure VACO has $\phi_w \approx 0.14$.

There is a dramatically different behavior in the scattering from the asphaltene nanoparticles when aggregation occurs in the incompatible blend: $I_L(\phi)$ has an upward curvature at low ϕ, as shown in Fig. 2(b). This unusual trend arises from the reduction in the concentration of nanoparticles in the incompatible region of mixing, since these nanoparticles are incorporated into the much larger aggregate structures. Therefore, we fit $I_L(\phi)$ to the hard sphere model in Fig. 2(b) only using the data in the range $0.7 \leqslant \phi \leqslant 1$, and extend the fitting results to low ϕ to show the behavior of $I_L(\phi)$ if no aggregation had occurred. From this, we estimate that SACO has $\phi_w \approx 0.20$. By assuming volume conservation of asphaltenes between the nanoparticles and aggregates, the difference between the fit and the data for $I_L(\phi)$ at low ϕ can be used to calculate the volume fraction of the aggregated asphaltenes, ϕ_{agg} as shown in Fig. 3(c). The initial rise in $\phi_{\mathrm{agg}}(\phi)$ is due to the blend's increasing asphaltene content, and the subsequent decrease beyond the peak at $\phi = 0.3$ reflects the increase in the blend's aromaticity and ability to solvate asphaltenes.

Larger asphaltene nanoparticles are more susceptible to aggregation than smaller asphaltene nanoparticles, as shown by comparing the ϕ dependence of the correlation length of the incompatible mixture to that of the compatible mixture. In the compatible mixture, the correlation length decreases systematically as ϕ increases [see Fig. 1(b) inset]; the structure factor effectively suppresses ξ at higher ϕ. Strikingly, $\xi(\phi)$ for the incompatible mixture exhibits a peak at $\phi = 0.5$ and decreases toward lower ϕ [see Fig. 2(b) inset]. This systematic decrease in the size of the asphaltene nanoparticles that remain in the mixtures after the aggregation has taken place is due to the reduction in the effective solvent quality for the asphaltenes as ϕ decreases and the surrounding oil becomes more aliphatic. This demonstrates that only the smaller asphaltene nanoparticles (i.e., maltenes) do not aggregate in the incompatible regime. These smaller asphaltenes do not interact as strongly with the other asphaltenes and can remain dispersed even in paraffinic oils.

A wealth of quantitative information about asphaltene nanoparticle aggregation in incompatible blends of whole crude oils can be garnered through SANS. The presence of a large I_{surf} that dominates I_L and I_{incoh}, power law exponents greater than the fractal threshold, $\alpha > 3$, the initial upward curvature in $I_L(\phi)$ which leads to nonzero ϕ_{agg}, and the peak in $\xi(\phi)$ are all hallmarks of aggregation and set boundaries on the range of ϕ for which the mixtures are incompatible. As can be seen from Fig. 3, all of these different criteria give the same incompatibility range for SACO-BPCO blends: $0 < \phi < 0.55$; this is confirmed by optical microscopy.

Given the molecular complexity of crude oils, it is remarkable that SANS can be used to study both asphaltene nanoparticles and aggregate structures in incompatible crude oil blends. The success of this approach is due to the significant neutron scattering contrast between the hydrogen-poor asphaltenes and the relatively hydrogen-rich liquid oil surrounding them. Performing SANS on natural crude oil blends and analyzing $I(q,\phi)$ provides a comprehensive quantitative picture of asphaltene structures and of oil compatibility. This approach may be extended to other colloidal dispersions such as nanoscale soot in motor oil in which aggregation is seen.

We thank D. Vega and A. Frischknecht for their help in the low q limit of the the hard sphere structure factor, and we thank W. Olmstead, M. Siskin, I. Wiehe, E. Sirota, R. Kennedy, B. Silbernagel, D. Siano, H. Deckman, C. Rebick, and H. Thomann for many stimulating discussions. We also thank the ExxonMobil PRT at NIST's Center for Neutron Research for the NG7-SANS beam time.

[1] K. H. Altgelt and M. M. Boduszynski, *Composition and Analysis of Heavy Petroleum Fractions* (Marcel Dekker, New York, 1994).

[2] B. P. Tissot and D. H. Welte, *Petroleum Formation and Occurrence* (Springer-Verlag, Berlin, 1984).

[3] R. Cimino, S. Correra, A. D. Bianco, and T. P. Lockhart, in *Asphaltenes: Fundamentals and Applications*, edited by E. Y. Sheu and O. C. Mullins (Plenum, New York, 1995).

[4] I. A. Wiehe and R. J. Kennedy, Energy Fuels **14**, 56 (2000).

[5] I. A. Wiehe and R. J. Kennedy, Energy Fuels **14**, 60 (2000).

[6] O. C. Mullins, in *Structure and Dynamics of Asphaltenes*, edited by O. C. Mullins and E. Y. Sheu (Plenum, New York, 1998), p. 21.

[7] S. I. Andersen, Energy Fuels **13**, 315 (1999).

[8] E. Y. Sheu, in *Structure and Dynamics of Asphaltenes*, edited by O. C. Mullins and E. Y. Sheu (Plenum, New York, 1998), p. 115.

[9] R. E. Ghosh and A. R. Rennie, J. Appl. Crystallogr. **32**, 1157 (1999).

[10] M. Y. Lin, E. B. Sirota, and H. Gang, Prepr. Pap.- Am. Chem. Soc., Div. Fuel Chem. **42**, 412 (1997).

[11] J. T. Koberstein, B. Morra, and R. S. Stein, J. Appl. Crystallogr. **13**, 34 (1980).

[12] N. W. Ashcroft and J. Lekner, Phys. Rev. **145**, 83 (1966).

[13] J.-P. Hansen and I. R. McDonald, *Theory of Simple Liquids* (Academic, London, 1986).